

LOW-FREQUENCY NOISE PREDICTION OF WIND TURBINES

Horia DUMITRESCU*, Florin FRUNZULICĂ**

* PhD, Professor, Institute of Statistics and Applied Mathematics, 13 September Street, Sect.V,
Bucharest, Romania, tel: +40 21.410.32.00/Int. 2718, e-mail: horiad@gheorghita.ima.ro
** Lecturer, PhD, Department of Aerospace Engineering, University "POLITEHNICA" of Bucharest,
1 Gh.Polizu Street, Sect.1, Romania, tel: +40 21.212.92.20, e-mail: ffrunzi@yahoo.com
** Researcher Assist., Institute of Statistics and Applied Mathematics, Bucharest, Romania

Three models that describe the influence of the tower on blade loading and noise generation have been implemented into a prescribed wake code. The models are validated with results of noise measurements. Impulsive low-frequency noise emission is computed for upwind and downwind turbines and a comparison is made between the two configurations. A variation of the main parameters shows their influence on noise generation. Load histories are presented as well.

Key words: Aerodynamic models, acoustic pressure, effect of blade thickness, blade loading, wind turbine.

1. INTRODUCTION

Impulsive low-frequency noise emissions of wind turbines can influence people although the frequency range is below the threshold of human hearing. Lowson [1] pointed out that it is even the most intense noise source for wind turbines in terms of radiated sound pressure. Hubbard and Shepherd [2] report measurements that show also the significance of low-frequency noise. These noise emissions are mainly caused by the blades passing the wake of the tower for the downwind configuration. The velocity deficit in the wake results in a sudden change in angle of attack that leads to a rapid decrease of torque and thrust. This load fluctuation causes an impulsive sound-pressure signal. A Fourier analysis reveals that the spectrum has highest sound-pressure levels (SPL) in the infrasound region of 1-20 Hz. In this work we will focus on this type of noise referred to as blade-tower-interaction noise (BTI).

Modern wind turbines have upwind rotors, i.e. the blade passes in front of the tower. Since there is no tower wake it could be assumed that BTI-noise model not occurs. This investigation follows to clarify this point.

2. AEROACOUSTIC ANALYSIS

2.1 Aerodynamic models

All calculations for this work were performed with a vortex-lattice method. It allows load and flow-field calculations of horizontal axis wind turbines and includes a prescribed-wake model [3].

Three models are incorporated into the code that describes the interaction of the blades with the tower for both upwind and downwind configuration. For upwind rotors the influence of the tower is often simulated by superposing a 2D dipole flow to the undisturbed flow. According to potential theory the result is a flow around a cylinder. Here the streamlines close behind the cylinder (fig.1a). The second model is the superposition of a 2D source flow to the undisturbed flow. The result is a flow around a semi-infinite body.

Here the streamlines do not close behind the tower, which is more realistic (fig.1b). However, this model does not hold downstream the tower because the flow is accelerated compared to the freestream velocity. Another approach lies in location of the source at half radius in upstream direction and choosing the source strength in such away that the stagnation point is on the tower surface (fig.1c). Hot-wire measurements of the velocity deficit in front of a tower were performed at a distance from the tower axis of 1.3 times the tower diameter for $Re \approx 0.23 \cdot 10^6$. Figure 2 shows measured data in comparison to the three potential theory models. The best agreement is found with the source location in upstream direction. All calculations for upwind configuration described below were done with this model.

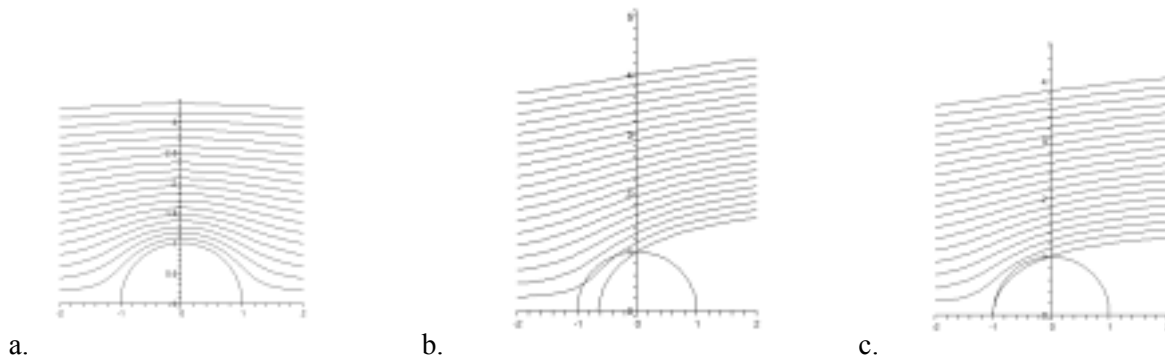


Fig. 1.

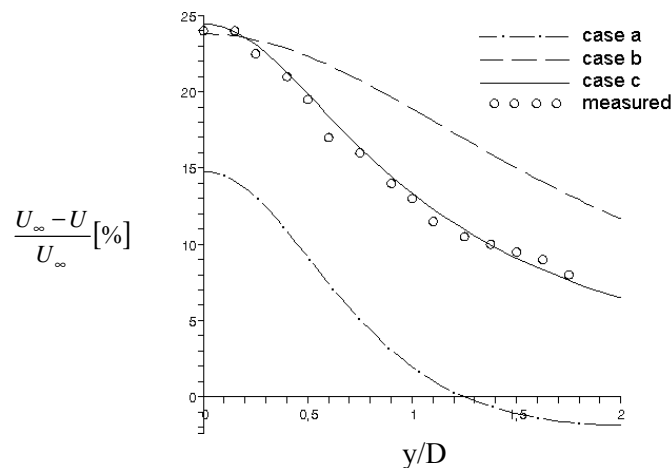


Fig. 2.

The flow field downstream the tower is viscous and cannot be modeled by potential flow. Therefore, measurements of the velocity defeat behind a circular tower had to be used.

A lot of measurements reported in literature are carried out for different Reynolds number and the tower shapes. Thus, ref. [4] gives measurements of velocity profiles as a function of distance to the tower for a circular cross-section tower of 3.9 m diameter at $Re = (1.6 - 3.0) \cdot 10^6$, ref. [5] gives wind tunnel measurements of the maximum velocity deficit, $\Delta U_{\max} / U_{\infty}$, behind the axis of a circular tower for $Re = 1.8 \cdot 10^6$, ref. [6] shows velocity profile measurements behind a circular tower in wind tunnel for $Re = 0.8 \cdot 10^6$. Comparison of these measurements shows that the maximum velocity deficit behind the tower axis increases with Reynolds number rise. This is consistent with the well-known increase of cylinder drag between $Re = (0.5 - 5) \cdot 10^6$. The velocity deficit in the wake of a tower and the velocity profiles are modeled by relations as

$$\frac{\Delta U_{\max}}{U_{\infty}} = C_1 \left(\frac{C_d \cdot D}{x} \right)^{1/2} \quad (1)$$

$$\frac{\Delta U}{\Delta U_{\max}} = \exp \left(-\frac{y^2}{C_2 \cdot x^2} \right) \quad (2)$$

where C_d (Re) is the drag coefficient, D is the diameter of tower, C_1 and C_2 are constants determined from experiment ($C_1 \cong 0.98$, $C_d \cong 0.55$, $C_2 \cong 0.113$).

The width of the wake is defined as the distance from the centerline where the tangent at the inflexion point intersects the axis of zero deficit (fig.3). The velocity deficit at this point amounts to 13.5% of the free stream velocity.

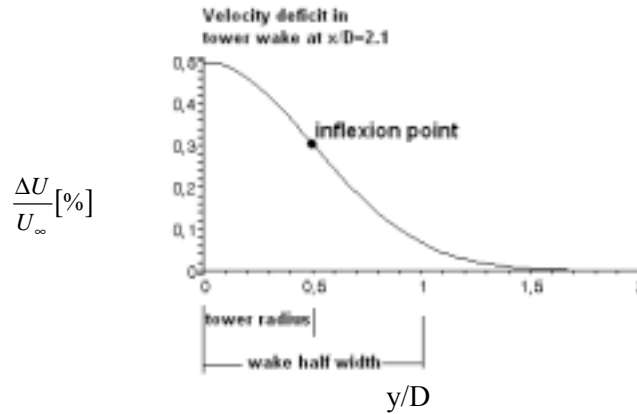


Fig. 3.

2.2 Aeroacoustic model

Once the load histories are known from the aerodynamic part they are used as input to the noise prediction model that is based on the approach of Succi [7]. Only thickness and loading noise terms are considered, whereas the quadruple terms that depend on turbulence in the field are neglected.

After some manipulations the Ffowcs Williams-Hawkings equation it is possible to express as

$$4\pi p(\vec{x}, t) = \underbrace{-\frac{\partial}{\partial x_i} \int_S \left[\frac{p_{ij} n_j}{r |1 - M_r|} \right] dS}_{\text{loading noise}} + \underbrace{\frac{\partial}{\partial t} \int_S \left[\frac{\rho_0 V_n}{r |1 - M_r|} \right] dS}_{\text{thickness noise}} \quad (3)$$

where S is the body surface, V_n denotes the source surface velocity normal to the surface, $p_{ij} n_j$ denotes the force per unit area acting from the surface onto to fluid, r is the distance between the source at \vec{y} and the observer at \vec{x} , and M_r is the relative velocity between the two divided by the speed of sound. All terms in square brackets have to be evaluated at the retarded source times, $\tau = t - r(\tau)/c$. Since the aerodynamic cod, based on the boundary element method, involves a discretization on the blade surface and assumes the local pressure distribution to be constant over the element, the pressure distribution can be replaced by equivalent force acting at the center of each element. Therefore the main input for the aeroacoustic calculation consists only of the forces and geometrical data of source, source motion, and observer. The concentrated forces and the blade volume act as compact acoustic sources. It is worth noting that the loading noise is produced by two effects: 1) motion of a force with constant magnitude relative to the observer; 2) change of the force magnitude and direction with respect to time.

The total acoustic pressure can be obtained by summing up the contributions of all sources n_s using the formulas given by Succi [7] and Farassat [8],

$$p(\vec{x}, t) = \sum_{i=1}^{n_s} p_{T,i}(t) + \sum_{i=1}^{n_s} p_{Ln,i}(t) + \sum_{i=1}^{n_s} p_{Lf,i}(t) \quad (4)$$

The source is located at the position \vec{y}_i and the observer at the location \vec{x} .

The three terms represent the effect of blade thickness $p_T(t)$, blade loading in the near field $p_{Ln}(t)$ and the far field $p_{Lf}(t)$. The following formulas give the contributions of every acoustic source, i.e. every panel, on the body surface. The thickness term is of monopole character and accounts for the displacement of the air by the blade element volume $V_{0,i}$:

$$p_{T,i}(t) = \frac{\rho_0 V_{0,i}}{4\pi} \left[\frac{1}{r} \frac{1}{1-M_r} \frac{\partial}{\partial \tau} \left(\frac{1}{1-M_r} \frac{\partial}{\partial \tau} \left(\frac{1}{1-M_r} \right) \right) \right] \quad (5)$$

The loading term is split into a near-field part

$$p_{Ln,i}(t) = \frac{1}{4\pi} \left[\frac{1}{(1-M_r)^2 r^2} \left(\vec{r}_i \cdot \vec{f}_i \frac{1-\vec{M}_i \cdot \vec{M}_i}{1-M_r} - \vec{f}_i \cdot \vec{M}_i \right) \right] \quad (6)$$

and a far-field part

$$p_{Lf,i}(t) = \frac{1}{4\pi} \left[\frac{1}{(1-M_r)^2 r} \left(\frac{\vec{r}_i}{c_0} \cdot \frac{\partial \vec{f}_i}{\partial \tau} + \frac{\vec{r}_i \cdot \vec{f}_i}{1-M_r} \left(\frac{\vec{r}_i}{c} \cdot \frac{\partial \vec{M}_i}{\partial \tau} \right) \right) \right] \quad (7)$$

It accounts for the noise generated by forces acting on the fluid, e.g. rotation of steady or fluctuating forces located on the rotor blade. The main parameters affecting the noise are the time-dependent force \vec{f}_i , the source Mach vector $\vec{M}_i = \frac{1}{c_0} \frac{\partial \vec{y}_i}{\partial \tau}$, its time derivative $\frac{\partial \vec{M}_i}{\partial \tau} = \frac{1}{c_0} \frac{\partial^2 \vec{y}_i}{\partial \tau^2}$ and the relative Mach number

$M_r = \frac{1}{c_0} \frac{\vec{x} - \vec{y}_i}{r} \cdot \frac{\partial^2 \vec{y}_i}{\partial \tau^2} = \vec{r}_i \cdot \vec{M}_i$ (the dimensionless speed of the source in the direction of the observer).

Further parameters are the distance to the observer $r = |\vec{x} - \vec{y}_i|$, mean air density ρ_0 , speed of sound c_0 , and blade segment volume $V_{0,i}$. All terms in square brackets have to be evaluated at retarded time, i.e. the noise is generated at source time τ and reaches the observer at the observer time t . Both times are related by:

$$t = \tau + r(\tau)/c_0 \quad (8)$$

Therefore, main advantages for this formulation are the ease of the computer coding and the speed of running, because the main input consist only the aerodynamic forces and geometrical data of source, source motion and observer.

3. RESULTS OF NOISE SIMULATION

3.1 Wind turbine configurations

Calculations were performed for two turbines: the Westinghouse WWG-0600 is a two-bladed upwind turbine with 600 kW rated power, a rotor diameter of 43.3 m, and a nominal rotational speed of 43 rpm [9];

the WTS-4 is a two-bladed downwind turbine 4200 kW rated power, a rotor diameter of 79.2 m and a nominal rotational speed of 30 rpm [10].

An important parameter for BTI-noise is the spacing between the blades and the tower, i.e. the distance between the rotor plane and the tower surface. For lack of detailed information, in the first case, we assumed a spacing of 2 m equal with the tower diameter. For the WTS-4 the spacing is 5.0 m at the blade root. Considering the blade cone angle the spacing at 70% radius is 7.7 m or 2.1 times the tower diameter of 3.66 m.

3.2 Comparison of measured and computed noise spectra

In a first step, the model was validated with measured data. Reference [9] reports measurements of SPL's for different wind speed and power output for the WWG-0600 turbine. Unexpected high experimental values in the infrasound region were explained by authors by means of sound possible inversion conditions in atmospheric boundary layer. However, calculations carried out in this work show that BTI-noise causes these SPL's. Simulation was done for two conditions: 500 kW power output at 10.3 m/s wind-speed and 600 kW at 13.0 m/s. The observer was located 65 m upwind the turbine. Figure 4 shows the computed narrowband spectra in comparison with measured data. Although the conditions for the first and second measurement were almost the same, there is a large difference up to 8 dB. Taking this into account, the agreement between measurement and calculation is good.

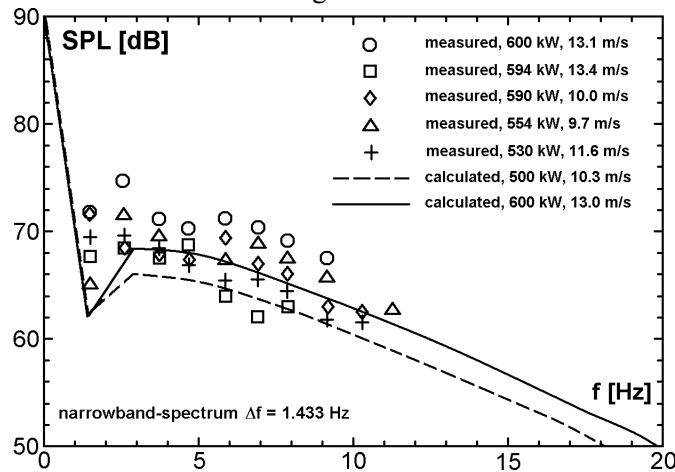


Fig. 4.

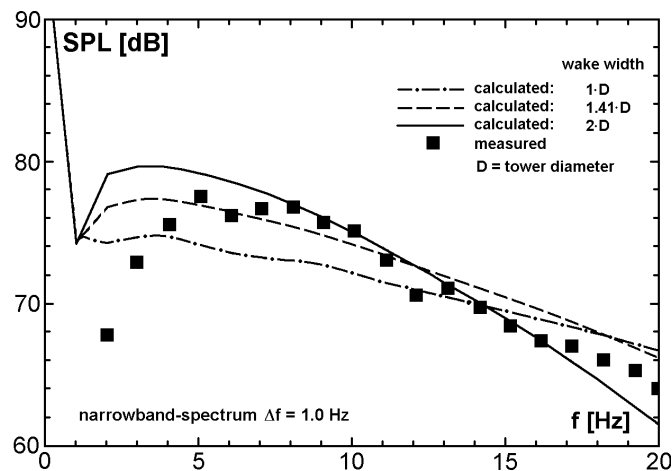


Fig. 5.

Reference [10] reports measurements of SPL's for the WTS-4 turbine. Comparison to measured data was performed for 2 MW power output at a wind speed of 12 m/s. The observer was located 91.5 m upwind the turbine. The Reynolds number for the flow around the tower was $Re \approx 30 \cdot 10^6$.

Figure 5 shows measured data together with the computed spectra for 3 Gaussian shaped wakes (eq.2) with different width. Best agreement is found for a wake with a width 2.0 times the tower diameter. The measured spectrum used for comparison with calculation was determined from a time signal that was 8 s long including about 8 sound-pressure pulses. Repeating the measurement for the same wind and power conditions might lead to a different spectrum due to the variation in tower wake caused by the vortices shed from the tower. In spite of this uncertainty the above described wake model is used for all further considerations.

3.3 Variation of configuration

Since both turbines operate at different power conditions, the BTI-noise generated by the upwind (WWG-0600) and downwind (WTS-4) configurations can not be compared directly. Therefore, simulations were repeated assuming that each turbine would operate in both configurations upwind and downwind. The spacing between blades and tower surface was kept the same, i.e. 1.0 times tower diameter for the upwind and 2.1 times tower diameter for the downwind configuration. Figure 6 a-b and 7 a-b show the sound-pressure signals and the narrow band-spectra for both turbines.

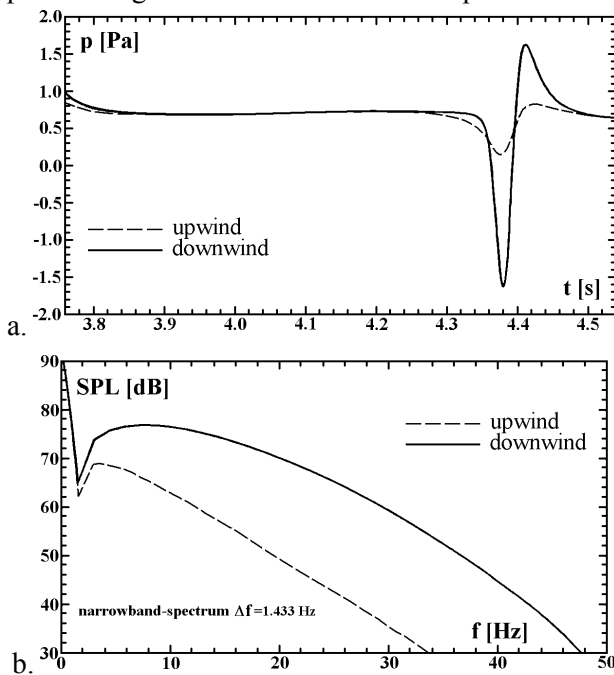


Fig. 6.

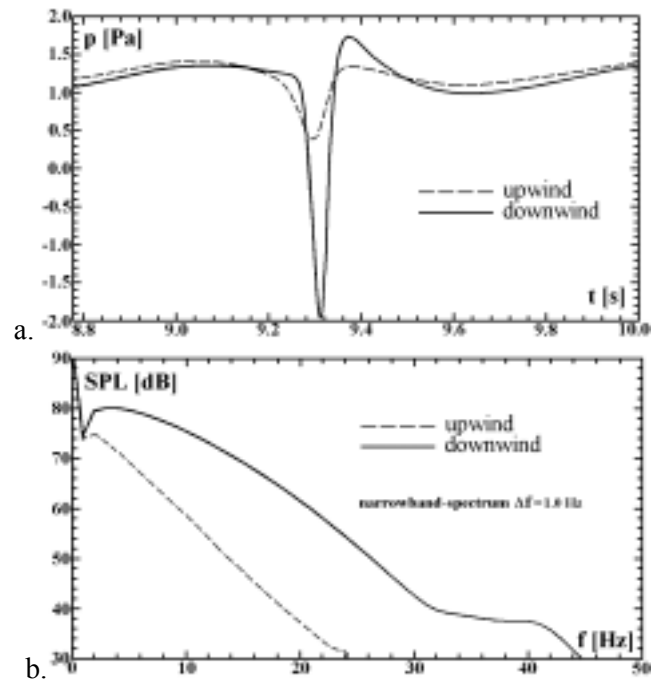


Fig. 7.

As expected, the sound-pressure signal is much sharper for the downwind configuration. For both turbines the amplitude peak, i.e. the difference between the maximum and minimum sound-pressure is 4 times higher for the downwind configuration than for the upwind configuration. The difference between the SPL's is 2-8 dB in the very low region below 5 Hz and about 20 dB in the region between 10 and 30 Hz. It is clear that an upwind turbine will radiate much less impulsive low-frequency noise than a downwind turbine.

Another main effect of blade-tower interaction is an additional dynamic blade loading which causes higher fatigue than would be expected when considering only the steady loading. Figure 8 a-b presents the comparison of the time variation of the total thrust force for both turbines in upwind and downwind configuration.

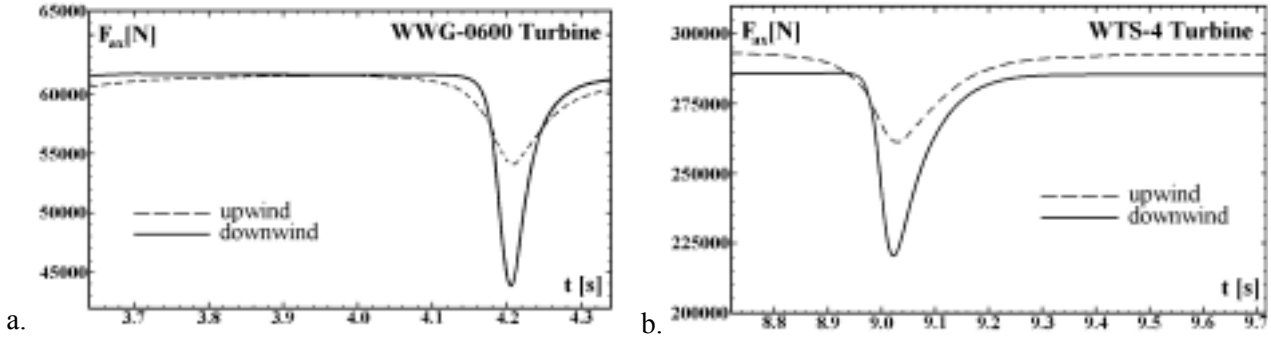


Fig. 8.

3.4 Variation of main parameters

For a given machine the important parameters for BTI-noise are the power output, the wind speed, the rotational speed, and the spacing between the blades and the tower surface. The influence of these parameters on the noise generation was investigated for the WWG-0600 turbine because most modern wind turbines will probably be upwind machines.

Reference point was the nominal rated power condition of 600 kW power output, 12.6 m/s, 43 rpm rotational speed, and 2 m spacing between blades and tower surface. For a given wind speed and rotational speed the power output was regulated by changing the pitch of the blades. The difference in total SPL compared to the reference case shows that the power output itself does not influence the noise generation in a conclusive way ($P = 500 \text{ kW}$, $\Delta p = 0.1 \text{ dB}$; $P = 700 \text{ kW}$, $\Delta p = -0.3 \text{ dB}$), whereas an increase of wind speed ($V_w = 10 \text{ m/s}$, $\Delta p = -1.2 \text{ dB}$; $V_w = 15 \text{ m/s}$, $\Delta p = 1.6 \text{ dB}$) and rotational speed ($\Omega = 38 \text{ rpm}$, $\Delta p = -1.5 \text{ dB}$; $\Omega = 48 \text{ rpm}$, $\Delta p = 2.0 \text{ dB}$) raises the total SPL and vice versa. For higher wind speeds the absolute value of the velocity deficit in front of the tower is greater which causes higher time-derivatives of the wind inflow as seen by the moving blade. In the same way a higher rotational speed leads to higher time-derivatives. This causes higher gradients in blade loading which yields higher SPL's according to aeroacoustic model. The reduced blade-tower spacing has also a great influence on noise generation, namely an increase of spacing reduces BTI-noise and vice versa ($\Delta z = 2.5 \text{ m}$, $\Delta p = -1.3 \text{ dB}$; $\Delta z = 1.5 \text{ m}$, $\Delta p = 2.3 \text{ dB}$).

4. CONCLUSIONS

A potential source-flow model is found to accurately describe the velocity deficit in front of a tower.

The often used 2D-dipol model underpredicts the velocity deficit. The computation of low-frequency blade-tower interaction noise is validated with the results of existent noise measurements for upwind and downwind turbines [9,10]. The agreement is found to be good.

A comparison of the upwind and downwind configuration shows that the maximum amplitude of the radiated pressure-pulse is four times higher for the downwind configuration. This pressure difference yields an increase of 10 dB. A parametric study for the upwind configuration reveals that BTI-noise is stronger for higher wind speeds, higher rotational speeds, lower blade-tower spacing and vice versa.

Passing the tower the blade suffers a decay in thrust force of 24% for the upwind configuration and about 50% for the downwind configuration.

Future work will include a more systematic investigation of BTI-noise and blade loads for different types of turbines and operating conditions. The aeroelastic effects on loads and BTI-noise will be considered as soon as the aeroelastic model is available.

REFERENCES

1. M.V. Lowson: *Applications of aero-acoustic analysis to wind turbine noise control*. *Journal of Wind Engineering*, vol.16,no.3, 1992, pp 126-140.
2. H.H. Hubbard, K.P. Shepherd: *Aeroacoustic of large wind turbines*. *Journal of the Acoustical Society of America*, vol. **89**, no.6, 1991, pp. 2495-2507.
3. H. Dumitrescu, F. Frunzulică: *A free-wake aerodynamic model for helicopter rotors*. *Proceedings of the Romanian Academy* (in press).
4. K. Barman, J.A. Dahlberg, S. Meijer: *Measurement of the tower wake of the Swedish prototype WECS Maglarp and calculations of its effect on noise and blade loading*. *Proceedings of the European Wind Energy Conference (EWEC)*, October 1994, pp. 56-63.
5. G. Schwarz, H. Knauss, H.Lienkart: *Nachlaufemtersuchungen für den Kaminturn des Aufwindkraftwerks Manzanares*. Internal Report, Institute für Aerodynamik und Gasdynamik, Universität Stuttgart, September, 1983, pp 1-28.
6. D. Althaus: *Vermessung der Nachlaufdelle eines Kreiszyllindres und eines symmetrischen Profils gleicher Dicke (Turm D/T=0.4) mit stufenweise abgeschnittener Hinterkante bei Nullanstellung*. Internal Report, Institute für Aerodynamik und Gasdynamik, Universität Stuttgart, June, 1983, pp 1-32.
7. G.P. Succi: *Design of quiet efficient propellers*. SAE Paper no. **790584**, 1979, pp 1-14.
8. F.Farassat: *Linear acoustic formulas for calculation of rotating blade noise*. *AIAA Journal*, vol. **19**, no.9, 1981, pp. 1122-1130.
9. K.P. Shepherd, H.H. Hubbard: *Noise radiation characteristics of the Westinghouse WWG-0600 (600 kW) wind turbine generator*. NASA TM-**101576**, July 1989, NASA Langley Research Center, pp 1-25.
10. K.P. Shepherd, H.H. Hubbard: *Measurements and observations of noise from a 4.2 MW (WTS-4) wind turbine generator*. NASA CR-**166124**, May 1983, pp 1-22.

Received October 14, 2004